Understanding the Recognition of Lewis X by Anti-Le^x Monoclonal Antibodies

Christopher J. Moore[†] *and France-Isabelle Auzanneau**

Department of Chemistry, University of Guelph, Guelph, Ontario, N1G 2W1, Canada;

KEYWORDS Tumor Associated Carbohydrate, ROESY, ELISA, H bond, Hydrophobic patch.

ABSTRACT

The recognition of the Le^x antigen by the anti-Le^x monoclonal antibody (mAb) SH1 was studied by ELISA using a panel of 4”-modified Le^x analogues. We confirmed that these analogues maintained the stacked conformation adopted by natural Le^x antigen using 1D ROESY experiments and measuring intramolecular distances. Our binding studies show that the 4-OH” of galactose behaves as an H-bond donor to an electronegative amino acid side chain in the SH1 binding site. While removal of this H-bond leads to reduced inhibition, disturbing the hydrophobic α face of the β-galactosyl residue leads to complete loss of binding to SH1. We compared our results to the crystal structure of the Fab fragment of anti-Le^x mAb 291-2G3-A complexed with Le^x (PDB entry code 1UZ8). While no H-bond involving the 4-OH” was described hydrophobic interactions between a tryptophan residue and the β-galactoside α face are

observed. We conclude that the hydrophobic α face that is uniquely displayed by β-galactosyl residues is essential to the recognition of the Le^x antigen by anti-Le^x antibodies.

INTRODUCTION

A large body of clinical and pre-clinical research has shown that antibodies raised in response to tumor-associated carbohydrate antigens (TACAs) can eliminate circulating tumor cells and micro-metastases.[1] Interestingly, fucose-containing glycosphingolipids were found to accumulate in gastric, colonic and lung adenocarcinomas while being virtually undetectable on normal gastric and colonic mucosa.[2] One such TACA is the hexasaccharide dimeric Le^x (dimLe^x, **1**) which accumulates in colonic and liver adenocarcinoma.[3] Many anti-Le^x mAbs such as FH2, FH3, SSEA1 and others were shown to react strongly with human adenocarcinoma.[2] However, since Le^x is also present on the surface of most normal epithelia cells these Abs also reacted strongly with normal granulocytes and kidney epithelia, and moderately with areas of the gastrointestinal epithelia.[4] A few selected mAbs, such as the IgG3 FH4, were found to recognize specifically polymeric-Le^x structures over monormeric Le^x.[3b] Following the discovery of FH4, two murine mAbs (IgG3) SH1 and SH2 were raised against the purified Le^x ceramide pentasaccharide LNFPIII (**2**) and the purified dimLe^x glycolipid (**1**), respectively.[3f] While anti-Le^x mAb SH1 was found to react strongly with the Le^x antigen, regardless of chain length; the anti-dimLe^x mAb SH2 only reacted strongly with dimLe^x and trimLe^x structures.[3f] Interestingly, anti-dimLe^x mAbs FH4 and SH2 have been shown

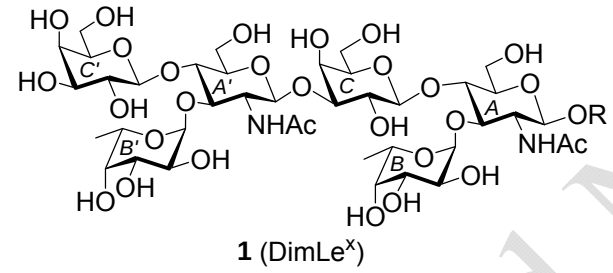

1 (DimLe^x)

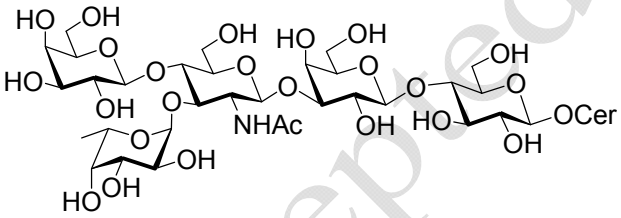

2 (LNFPIII)

to selectively immunostain adenocarcinoma cells while they showed very limited staining of normal adult cells.[3b] In this context, we are attempting to design an anticancer vaccine based on the dimLe^x hexasaccharide **1**. An important factor to consider is that a vaccine composed of the native dimLe^x antigen would also elicit an immune response against the Le^x determinant (SH1-like antibodies), which would ultimately lead to the destruction of healthy cells. Thus our primary goal has been to discover dimLe^x analogues that retain the internal epitope recognized by anti-dimLe^x SH2-like antibodies but do not display the epitope recognized by anti-Le^x SH1-like antibodies. We have synthesized various Le^{x}OMe analogues in which L-fucose was replaced by L-rhamnose and D-galactose and *N*-acetylglucosamine were replaced by D-glucose.[5] Stochastic searches and NMR experiments[6] confirmed that such analogues adopted the preferred stacked conformation that has been identified for the natural Le^x trisaccharide[6-7] and the binding affinity of these analogues for the anti-Le^x mAb SH1 was examined by competitive ELISA.[6] We discovered that the analogue in which the galactose unit was replaced by a glucose (**3**) residue displayed no binding to the SH1 mAb, even at high concentrations. Based on what is known about protein-carbohydrate recognition,[8] the loss of binding between SH1 and GlcLe^x (**3**) may result from either a) the presence of the Glc 4-OH within the α face of what used to be an exposed hydrophobic patch in the β-galactosyl residue;[8b] b) a difference in solvation of the

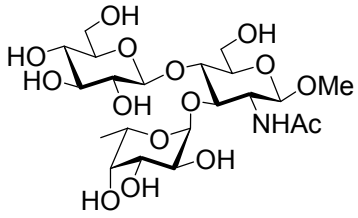

3 (GlcLe^{x}OMe)

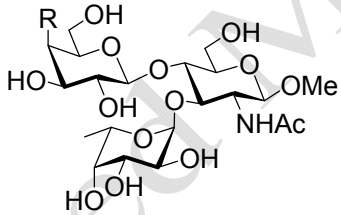

4 R = OH, (Le^{x}OMe)
5 R = OMe
6 R = H
7 R = Cl
8 R = F

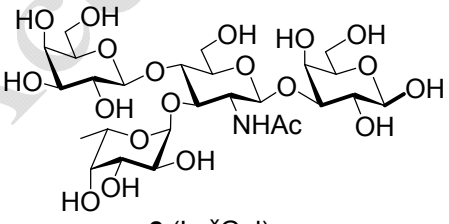

9 (Le^{x}Gal)

analogue *vs.* that of Le^x; or c) the loss of a strong H-bond involving the axial 4"-OH group in Le^x. In this paper, we attempt to shed light on the involvement of the 4"-OH group in Le^xOMe (**4**) to the binding of this antigen with mAb SH1. To this end, we used four described[9] Le^xOMe analogues (**5**–**8**) in which the 4"-OH was replaced with a methoxy (**5**, 4"-methoxy Le^xOMe), a hydrogen (**6**, 4"-deoxy Le^xOMe), a chlorine (**7**, 4"-deoxychloro Le^xOMe) or a fluorine (**8**, 4"-deoxyfluoro Le^xOMe). We also measured the binding affinity of SH1 for tetrasaccharide **9** (Le^xGal) provided by Samain et al.[10] To ensure that any conclusion drawn from the binding experiments did not result from a change of conformational behavior of the Le^x analogues, we also assessed the conformation of analogue **5**–**8** by NMR.

RESULTS AND DISCUSSION

Conformational Study of analogues 5–8 by NMR. It has been well-established that the Le^x trisaccharide was a rather rigid structure which adopted the so-called "stacked conformation"[6-7] shown on Figure 1.

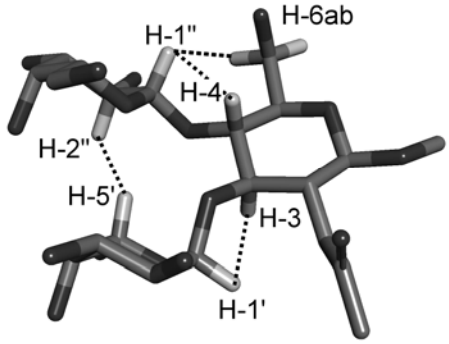

Figure 1: Close contacts in the global minimum conformation known[6,7d,e] for the Le^x trisaccharide.

This conformation is characterized by NOE contacts between the fucosyl H-1' and GlcNAc H-3, the galactosyl H-1" and GlcNAc H-4, H-6a and H-6b, and most importantly between the

Table 1 Proton chemical shifts (ppm) at 600 MHz (300 K) in D_2O.

	5	**6**	**7**	**8**
H-1	4.48	4.48	4.48	4.48
H-2	3.90	3.91	3.92	3.90
H-3	3.85	3.87	3.89	3.87
H-4	3.89	3.91	3.92	3.93
H-5	3.59	3.60	3.60	3.60
H-6a	4.00	4.02	4.02	4.01
H-6b	3.85	3.89	3.88	3.87
H-1’	5.09	5.11	5.12	5.10
H-2’	3.69	3.70	3.71	3.69
H-3’	3.90	3.90	3.88	3.87
H-4’	3.76	3.78	3.86	3.73
H-5’	4.82	4.82	4.77	4.80
H-6’(3H)	1.18	1.20	1.20	1.17
H-1”	4.42	4.45	4.52	4.54
H-2”	3.44	3.12	3.51	3.50
H-3”	3.67	3.76	3.97	3.79
H-4”	3.54	(ax) 1.25 (eq) 2.00	4.60	4.82
H-5”	3.61	3.65	3.91	3.74
H-6a”	3.76	3.62	3.81	3.75
H-6b”	3.76	3.56	3.72	3.75

fucosyl H-5’ and the galactosyl H-2”. [6,7d,e] To assess whether analogues **5**–**8**[9] maintained this stacked conformation despite being modified at C-4 of galactose, we measured inter-proton distances using 1D ROESY experiments. The ^{1}H chemical shifts were first assigned for trisaccharides **5**–**8** using a combination of ^{1}H, COSY, HSQC, JMOD and TOCSY experiments and are reported in Table 1. The vicinal coupling constants measured for the three sugar units supported, as expected, an average $^4C_1$ conformation for the 4-OMe, 4-deoxy, 4-deoxychloro and 4-deoxyfluoro galactose rings as well as for the *N*-acetylglucosamine residue. The $^1C_4$ conformation of the fucosyl rings in all analogues was also supported by the vicinal coupling constants. Inter-residue NOE interactions were evaluated at 300 K selectively irradiating H-1’, H-1” and H-5’ for each analogue. We show in Figure 2 the ^{1}H NMR spectrum and the ^{1}H, ^{1}H ROESY spectra (mixing time 100 ms) acquired at 600 MHz

on a cryoprobe-equipped spectrometer for analogues **5**–**8**. For all analogues, the expected inter-residue cross-relaxation signals were evident.

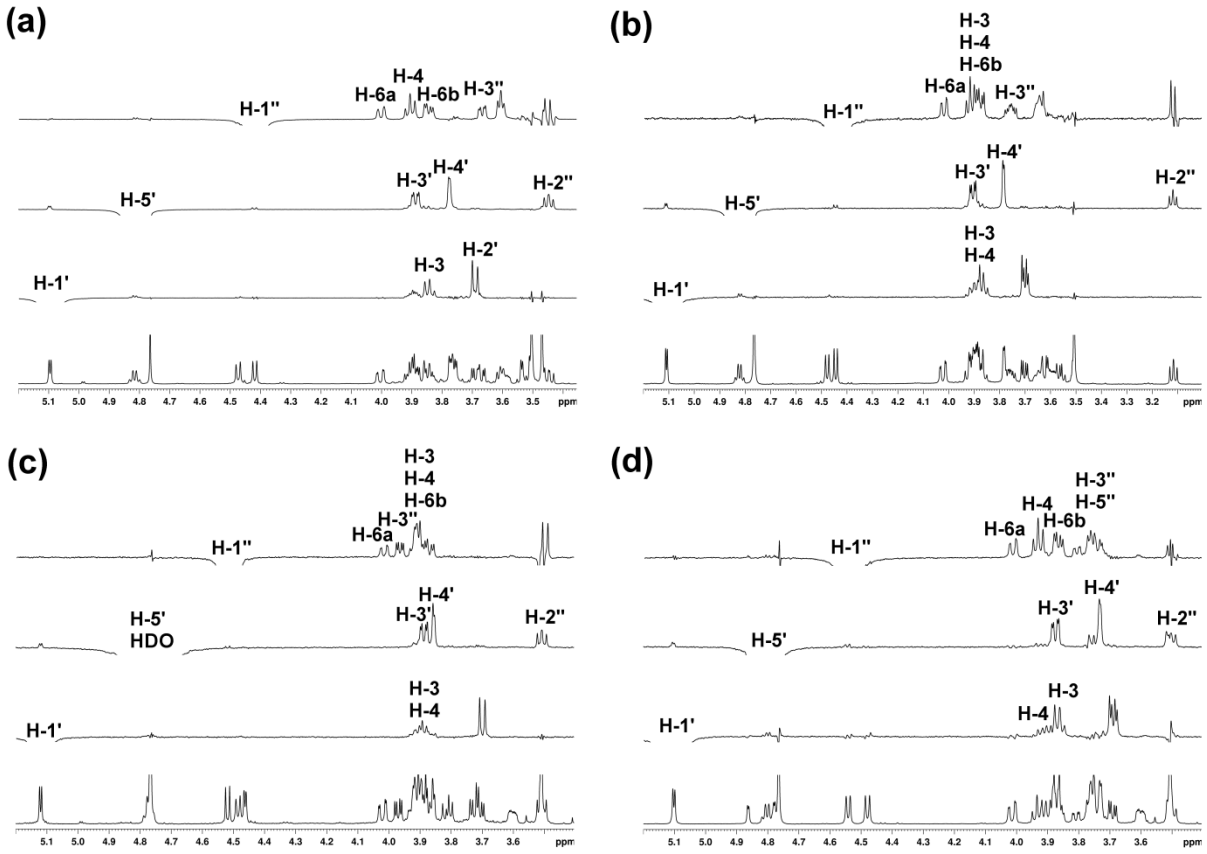

Figure 2: ^{1}H NMR spectra (600 MHz, 300 K) and ^{1}H, ^{1}H ROESY spectra (mixing time 100 ms) a) trisaccharide **5**: selective excitations of proton H-1' and H-5' and H-1''; b) trisaccharide **6**: selective excitations of proton H-1', H-5' and H-1''; c) trisaccharide **7**: selective excitation of proton H-1' and H-1'', combined excitation of H-5' and the residual solvent signal; d) trisaccharide **8**: selective excitations of proton H-1', H-1'' and H-5'.

For analogue **7** the H-5' signal was found to overlap with the residual HDO signal, thus these signals were irradiated together and gave the expected cross relaxation signal to H-2'' galactose.

Cross-relaxation buildup curves for those well-resolved signals were obtained acquiring experiments over 7 mixing times ranging from 40 ms to 200 ms with 4 mixing times below 100 ms to ensure accurate fit of the double exponential equations at low mixing times (Figure 3).

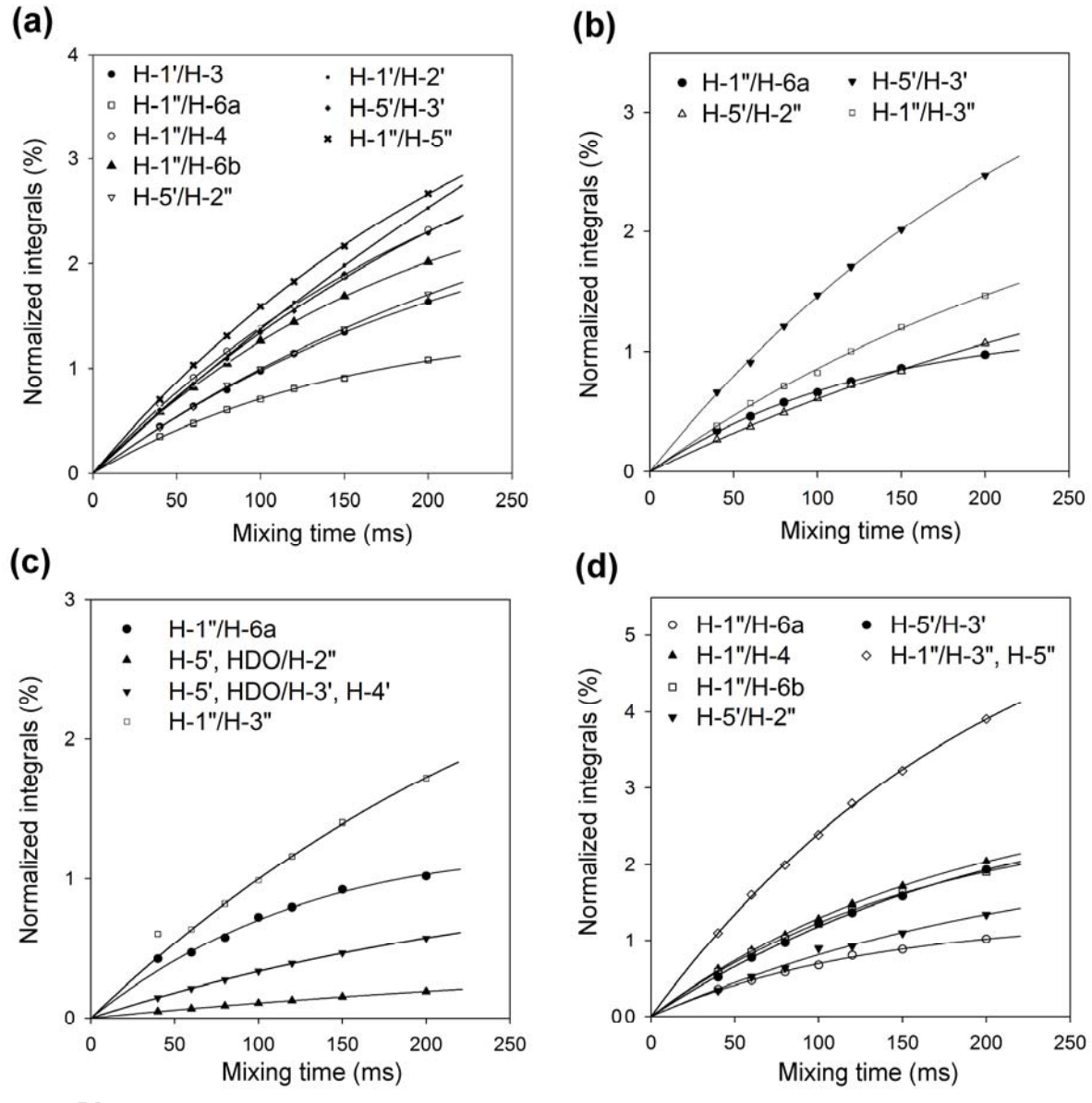

Figure 3: ^{1}H, ^{1}H ROESY buildup curves a) trisaccharide **5**: selective excitations of H-1', H-1" and H-5'; b) trisaccharide **6**: selective excitations of H-1" and H-5'; c) trisaccharide **7**: selective excitation of H-1", combined excitation of H-5' and residual solvent signal (HDO); d) trisaccharide **8**: selective excitations of H-1" and H-5'.

The normalized buildup curves were fitted to double exponential equations [$f(\tau_m) = A[\exp(B\tau_m) - \exp(C\tau_m)]$. The initial slopes at 0 ms mixing times were then calculated from the first derivatives [$f'(0) = A(B-C)$] and used to evaluate inter-proton distances using the isolated spin pair approximation.[11] In two instances (irradiations of H-5' in the 4"-deoxychloro analogue **7** and H-1" in the 4"-deoxyfluoro analogue **8**) the reference signals used for distance calculations resulted from the combination of overlapping contributions from two known short distances and were treated as such. In all cases the R^2 values for the exponential fits were at least 0.97. The measured inter-proton distances for the glycosidic linkages (H-1′ to H-3, H-1" to H-4) and between H-2' to H-5", as well as the distances measured from H-1" to H-6a and H-6b are given in Table 2. We also list in Table 2 the distances that we have reported for the Le^xOMe (**4**) trisaccharide and that are supporting the stacked conformation for this branched trisaccharide.[6] As can be seen in this table, the distances measured for the 4"-modified analogues **5**–**8** are in good agreement with that measured for the Le^x methyl glycoside **4**.

Table 2: Measured[a] distances (Å) for Le^xOMe[6] (**4**) and analogues **5**–**8**.

	4[b]	**5**	**6**	**7**	**8**
H-1'/H-3	_[c]	2.54	_[c]	_[c]	_[c]
H-5'/H-2"	2.66	2.62	2.73	2.58	2.60
H-1"/H-4	2.44	_[c]	_[c]	_[c]	2.45
H-1"/H-6a	2.69	2.71	2.62	2.75	2.68
H-1"/H-6b	2.49	2.50	_[c]	_[c]	2.47

[a] $r_{ij} = r_{ref} (S_{ref}/S_{ij})^{1/6}$. [b] Reported.[6] [c] Signal overlap precluded measurement.

In particular the inter-residue distances measured between the fucosyl H-5' and the galactosyl H-2" are consistent throughout the series of analogues. Thus, this NMR data indicates that analogues **5**–**8** also adopt the stacked conformation known for the Le^x antigen.

As mentioned above, the fucosyl H-5' signal overlapped with the HDO signal in analogue **7** (see Figure 2c) and a combined excitation of both signal showed the expected cross-relaxation

signals to H-3’ and H-4’ as well as to H-2”. When looking at the corresponding buildup curves (Figure 3c, ▲ and ▼), one observes that only up to 0.2% and up to 0.6% signal were obtained at the longer mixing times. We assumed that this apparent low cross relaxation resulted from the combined irradiation of H-5’ with HDO and the normalization against these combined signals. To support this hypothesis, 1D ROESY experiments were acquired at 307 K to shift the HDO signal upfield thus allowing the selective irradiation of H-5’ (Figure 4). Indeed, as can be seen on Figure 4b, with a mixing time of 150 ms cross relaxation was greater than 1% between H-5’ and H-2” while cross relaxation from H-5’ to H-3’ and H-4’ combined was more than 3%. Data was acquired over 5 mixing times and the slopes at initial buildup were used to measure the distance between H-5’ and H-2” at 307 K. Even though this distance of 2.70 Å appeared to be slightly longer than that measured at 300 K (Table 2) it is still in excellent agreement with the 4”-deoxychloro analogue **7** adopting preferentially the stacked conformation at 307 K.

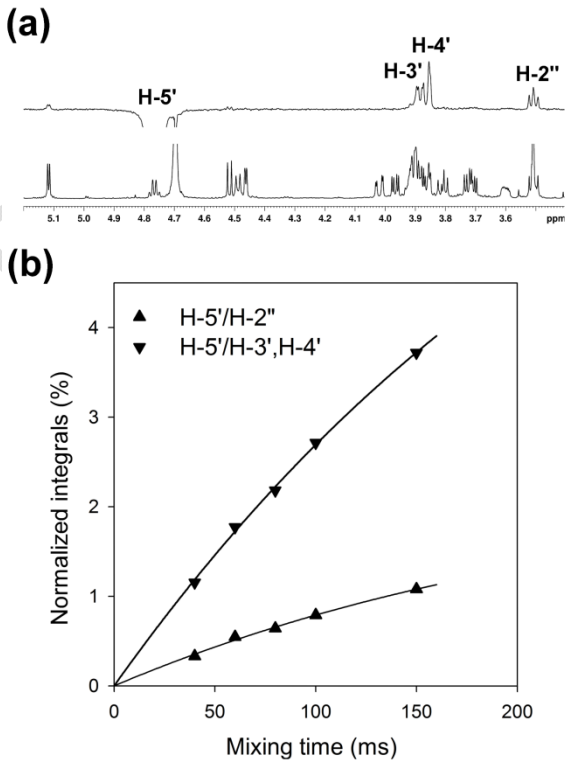

Figure 4: a) Trisaccharide **7**, ^{1}H NMR spectra and ^{1}H, ^{1}H ROESY spectra at 307 K (600 MHz) upon selective excitation of H-5' (100 ms); b) cross relaxation buildup curves.

Having established that all analogues maintained a similar conformational behavior to that of the natural Le^x trisaccharide, we carried out binding experiment with the mAb SH1 to assess if the modification at C-4" had an impact on recognition by this antibody.

Binding Studies with analogues 4–9 and mAb SH1. The affinity of the anti-Le^x monoclonal antibody SH1[3f] for Le^x (**4**)[5b] was compared to its affinity for the analogues **5**–**8**[9] by competitive ELISA experiments using Le^x trisaccharide-BSA[6] **10** as the immobilized competing ligand.[12]

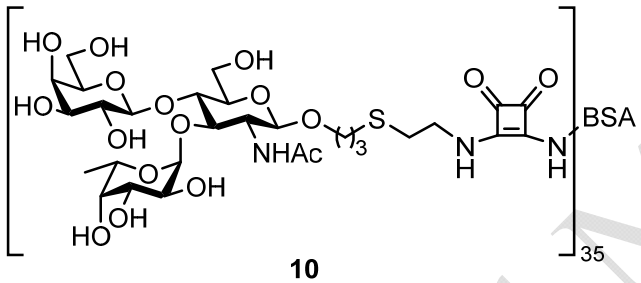

10

We also measured the binding affinity of SH1 for Le^x-Gal **9** provided by Samain et al.[10] Tetrasaccharide **9** was then used as internal standard on all ELISA experiments performed with analogues **5**–**8**. The average IC_{50} measured for analogue **9** over all experiments was 256 μM with a standard deviation of ± 5 μM which confirmed the reliability of the experiments. Percent inhibition was plotted against inhibitor concentration and fitted to a 4 parameter logistics sigmoidal equation (Figure 5) and we determined the concentration of each analogue required for 50% inhibition (IC_{50}) of the Le^x-SH1 binding. The measured IC_{50} and corresponding calculated Δ(ΔG) using Le^{x}OMe as a reference are given in Table 3. Tetrasaccharide Le^{x}Gal had a slightly higher affinity for the antibody than the Le^{x}OMe trisaccharide indicating that the galactose residue at the reducing end of Le^x interacts favorably with the periphery of the antibody binding site. The 4"-methoxy Le^x analogue **5** showed no inhibition of the Le^x binding to SH1, even at high concentrations (››18 mM) suggesting that the methyl group led to unfavorable steric interactions within the binding site. Removal of the

hydroxyl group in 4”-deoxy analogue **6** resulted in a loss in binding of 1.3 kcal.mol^{-1} that is consistent with the loss of a hydrogen bond between the ligand and the combining site.[8a,13]

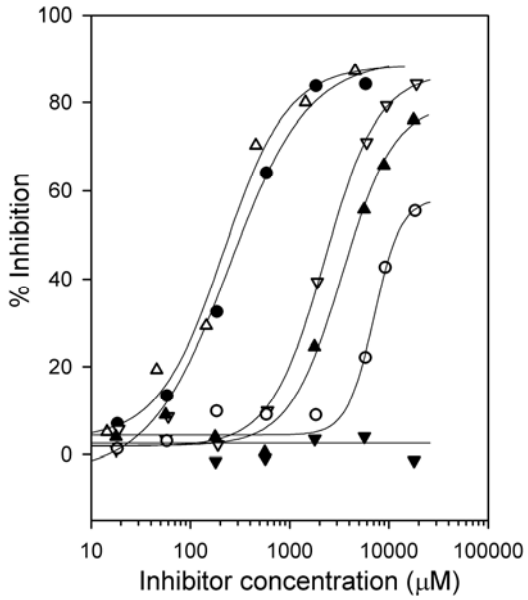

Figure 5. Inhibition curves for MAb SH1 using Le^x-BSA^6 as immobilized antigen and analogues **4**–**9** as soluble competitive inhibitors: **4** (●), **5** (▼), **6** (▽), **7** (▲), **8** (○), **9** (△).

The inhibition results obtained with the 4”-deoxyhalo analogues **7** and **8** allow us to speculate whether the axial 4”-OH on Le^x behaves as a hydrogen donor or acceptor in the formation of an H-bond in the SH1 binding site.[8a,14] The 4”-deoxychloro analogue **7** was a much weaker competitor than the native Le^x antigen (Δ(ΔG) of 1.6 kcal mol-1) suggesting that the axial 4”-OH in Le^x donates a hydrogen to the formation of an H-bond with an amino acid side chain in the binding site. The 4”-deoxyfluoro analogue **8** led to a much greater loss in binding than the chloro analogue **7** (Table 3 compare entries 5 and 6). This result is consistent with the observation made by Vermersch et al.[15] that replacement of a H-bond donor hydroxyl group by a fluorine atom may lead to destabilization of the complex through electrostatic repulsion between the

electronegative H-bond acceptor amino acid side chain and the very electronegative fluorine atom.

The results obtained for the 4”-deoxy Le^x analogue **6** together with that obtained with the chloro and fluoro analogues **7** and **8** indicate that the 4”-OH in Le^x is donating a hydrogen to the formation of an H-bond with an electronegative amino acid side chain in the binding site. However, the replacement of the galactose residue in Le^x with a glucose unit (**3**) resulted in no inhibition of Le^x binding to the SH1 antibody[6] which cannot be explained by only the loss of a H-bond. We conclude that not only a hydrogen bond contact with SH1 is destroyed, but that the equatorial hydroxyl group in $GlcLe^x$ **3** creates unfavorable electrostatic interactions with the antibody binding pocket by pointing within the hydrophobic galactosyl α face that is normally present in the natural Le^x antigen.[6]

Table 3: Inhibition data for MAb SH1with analogues **4–9**.

Entry	Inhibitor	IC_{50}[a] (μM)	$\Delta(\Delta G)$[b] (kcal mol^{-1})
1	**4** (Le^xOMe)	337	0
2	**9** (Le^xGal)	256 ± 5	-0.2 ± 2%
3	**5** (4”-methoxy)	››18000	–[c]
4	**6** (4”-deoxy)	2933	1.3
5	**7** (4”-deoxychloro)	4838	1.6
6	**8** (4”-deoxyfluoro)	11685	2.1

[a] Concentration of inhibitor required for 50% inhibition using solid phase glycoconjugate **10** as immobilized antigen. [b] Values determined from the expression $\Delta(\Delta G) = RT \ln([I_1]/[I_2]$ where $[I_2]$ is the IC_{50} measured for the reference inhibitor Le^xOMe **4** and $[I_1]$ the IC_{50} measured for each analogue **5–9** with R = 1.98 $cal.K^{-1}$and T = 296 K. [c] No inhibition observed at 18 mM.

Comparison with anti-Le^x mAbs IG5F6 and 291-2G3-A. To gain understanding on the interaction between anti-Le^x antibodies and the Le^x antigen when the trisaccharide epitope is displayed at the reducing end of polymeric Le^x oligosaccharides, it is

useful to review the recent contributions by Altman et al.[16] on *Helicobacter pylori* lipopolysaccharides (LPSs) and those of van Roon et al. [17] on parasitic schistosomes.

It is known that *O*-chains of *H. pylori* LPSs from a variety of different isolates express the Le^x antigen[18] and that *H. pylori*-induced antibodies cross-react with gastric mucosa of both humans and mice causing atrophic gastritis and adverse autoimmune reactions.[19] In a recent study, Altman et al. infected mice with *H. pylori* strain O:3.[16] and cloned mAb IG5F6 (IgG3) which was found to be specific for the Le^x antigen. The dissociation constants for oligosaccharides LNFPIII, $dimLe^x$ and $trimLe^x$ binding to immobilized IG5F6 were measured by SPR to be 55 μM, 42 μM and 28 μM, respectively. Thus, mAb IG5F6 shows higher affinity for polymeric Le^x structures, suggesting that polymeric Le^x oligosaccharides are immunodominant over the terminal non-reducing end Le^x trisaccharide in this *H. pylori* LPS.

Parasitic schistosomes are also known to express Le^x on glycolipids and glycoproteins, both in its monomeric and polymeric form.[20] In their study, van Roon et al. infected mice with *Schistosoma mansoni* cercariae and showed that the sera of infected mice presented detectable antibody responses against LNFPIII, $dimLe^x$ and $trimLe^x$ from 2 weeks onwards.[17c] Here again, the binding to oligomeric Le^x was greater than that against LNFPIII suggesting that epitopes presented within polymeric Le^x structures were immunodominant. MAb 291-2G3-A (IgG3) was shown to recognized both Le^x and polymeric Le^x (ref.[17a]) and the X ray structure of its Fab fragment with the Le^x trisaccharide was solved (PDB entry code 1UZ8).[17a,b] In this particular complex, no H-bond involving the 4-OH" of galactose was observed but a tryptophan residue (Trp 33) is seen to form favorable aromatic stacking interactions;[8b,17b] with the hydrophobic patch of the galactosyl α face (Figure 6).

These results taken collectively clearly illustrate that different groups of antibodies are evoked depending on the presentation of Le^x to the immune system. While mAbs 1G5F6 and 291-2G3-A do recognize the LNFPIII pentasaccharide that displays monomeric Le^x, their binding affinities for dimLe^x was somewhat higher.[16,17b] We conclude that mAb 1G5F6 and 291-2G3-A were raised predominantly against epitopes displayed by polymeric Le^x structures. These mAb in turn recognize epitopes that are somewhat extended from the terminal Le^x trisaccharide, rather than epitopes strictly localized on the non-reducing end trisaccharide. In contrast, since SH1 was raised against the monomeric Le^x pentasaccharide (LNFPIII, **2**) it recognizes an epitope more localized to the trisaccharide and that only moderately extends towards the lactosamine residue as supported by it slightly higher affinity for tetrasaccharide **9**.

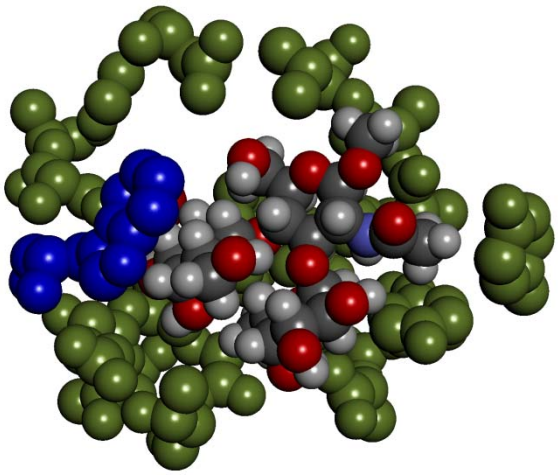

Figure 6. Crystal structure (PDB entry code 1UZ8): binding site of Fab fragment of mAb 291-2G3-A with Le^x,[17a,b] showing Trp 33 (blue) forming favorable stacking interactions with the Le^x galactosyl hydrophobic α face.

CONCLUSION

In conclusion, the binding strength of anti-Le^x mAb SH1 to the 4”-manipulated Le^xOMe analogues **5**–**8** follows the order 4”-deoxy > 4”-deoxychloro > 4”-deoxyfluoro > 4”-methoxy.

Changes in free energy of binding compared to the native Le^x antigen allowed us to conclude that the lack of recognition of mAb SH1 for analogue **3** ($GlcLe^xOMe$) results from the abolition of a hydrogen bond involving the 4-OH" as well as unfavorable electrostatic interactions in the antibody binding pocket as the equatorial OH group disturbs what used to be the hydrophobic patch of the β-galactosyl α face. Since no H-bond involving 4"-OH is seen in the crystal structure of the complex Le^x/mAb 291-2G3-A Fab fragment, we also conclude that SH1 binds Le^x in a different manner than anti-Le^x mAb 291-2G3-A. However, favorable aromatic stacking interactions between a tryptophan residue (Trp 33) and the hydrophobic patch of the galactosyl residue α face (Figure 6) suggest that the $GlcLe^xOMe$ analogue **3** would not bind to this mAb either. Thus the β-galactoside in Le^x is shown here to be a key residue for recognition of the Le^x antigen by anti-Le^x antibodies. More specifically, the presence of an axial hydroxyl group at C-4" able to donate an hydrogen to H-bond formation and most importantly the presence of the characteristic galactosyl α face hydrophobic patch are the main features that drive the specific binding and anti-Le^x antibodies to Le^x. Since analogues of Le^x in which the galactose residue is replaced by glucose do not display these essential features not only binding to anti-Le^x antibodies is abolished but we propose that such analogues will not either trigger the production of antibodies that are able to bind to the Le^x natural antigen. Immunizations studies with a synthetic[21] analogue of $dimLe^x$ in which the non-reducing end galactose residue is replaced by a glucose unit are on-going in our laboratory. Given that the analogue does not display the hydrophobic α patch nor the axial hydroxyl group typical of the β-galactosyl residue, we expect that it will not trigger the production of SH1- or 291-2G3-A-like antibodies and hope that, in contrast, it will trigger the production of FH4- or SH2- like antibodies that specifically recognize internal epitopes displayed by polymeric Le^x at the surface of cancer cells.

EXPERIMENTAL SECTION

General Section. The syntheses of the Le^{x}OMe (**4**) and analogues **5**–**9** used in this study were previously reported.[5b,9,10] All compounds were purified by gel permeation chromatography on Biogel P2 and characterized by NMR and ESIMS. Their purity was estimated to be >95% in all cases. Preparation of glycoconjugate **10** was also reported[6] the degree of incorporation of Le^x was assessed by the Dubois colorimetric assay.[22]

NMR Experiments. The trisaccharides **5**–**8** (4–7 mg) were lyophilized from D_2O (99%, 3 mL) and dissolved in 0.7 mL of D_2O (99.96%). The solutions were immediately transferred to 5 mm NMR tubes which were carefully sealed with parafilm. One-dimensional selective gradient ROESY experiments were acquired at 300 K using a 600 MHz spectrometer equipped with a cryoprobe following selective excitations of protons: H-1', H-1" and H-5" and applying a 5 s relaxation delay between scans. For analogue **7**, additional experiments were carried out at 307 K, with selective irradiation of H-5' and H-1". The optimum irradiation range for each signal was used to determine the best length of the soft pulse applied. This value was automatically calculated by Bruker software (BUTSEL-NMR). 1D ROESY spectra were recorded at 5–7 mixing times from ranging 40 ms to 200 ms. Before Fourier transformation, the FIDs were zero-filled once and multiplied with a 1 Hz line broadening factor. Spectra were phase and baseline corrected and integrated. The integrals measured for the irradiated signals were plotted against mixing time and the obtained curves were fitted to a double exponential decaying function:

$$f(\tau_m) = -A[\exp(B\tau_m) + \exp(C\tau_m)]$$

where τ_m is the mixing time and A, B and C are adjustable parameters. The values of these integrals were extrapolated to 0 ms mixing time, and the integrals from cross-relaxation peaks were normalized through division by these extrapolated values. The normalized cross-relaxation

integrals were plotted against the mixing times and the buildup curves were fitted to a double exponential equation of the form

$f(\tau_m) = A[\exp(B\tau_m) - \exp(C\tau_m)]$

the initial slopes at 0 ms mixing times were determined from the calculated first derivatives[11]

$f'(0) = A(B\text{-}C)$

Interproton distances were calculated based on the isolated spin pair approximation (ISPA):

$r_{ij} = r_{ref}(S_{ref}/S_{ij})^{1/6}$

where S is the initial slope at $\tau_m = 0$, and r is the proton-proton distance.

The intra-residue cross-peaks used as reference for distance determinations were:

For analogue **5**: references H-1'/H-2' (2.42 Å), H-5'/H-3' (2.47 Å) and H-1"/H-5" (2.42 Å).

For analogue **6**: references H-5'/H-3' (2.47 Å) and H-1"/H-3" (2.60 Å).

For analogue **7** at both 300 K and 307 K: references combined H-5'/H-3' (2.47 Å) with H5'/ H-4' (2.43 Å), and H-1"/H-3" (2.60 Å).

For analogue **8**: references H-5'/H-3' (2.47 Å) and combined H-1"/H-3" (2.60) with H-1"/H-5" (2.42 Å).

Competitive ELISA procedures. A NUNC 96-well ELISA microtiter plate was coated with a dilution of the Le^x-BSA glycoconjugate **10** (100 µL per well, 4 µg/mL) in a 0.05 M carbonate-bicarbonate buffer at pH 9.6. The plate was covered with Saran wrap and incubated at 4 °C for 16 h. The antigen solution was discarded and the plate was washed (3 x 5 min incubation periods with buffer) with a PBS buffer at pH 7.4 containing 0.05% Tween 20. The plate was then rinsed with PBS and blocked with skim milk (DIFCO, 5% in PBS-0.05% Tween 20, 400 µL per well). After a 1 h incubation at 37 °C, the plate was rinsed (3x) with PBS. Each well received a solution containing 50 µL of competitor (concentration range from 0.2 µg/mL to 20 mg/mL in 2% skim

milk in PBS) and 50 μL of a solution of SH1 antibodies (1:125 dilution in 2% skim milk in PBS). The plate was incubated for 3 h at 23 °C. The plate was subsequently washed (3 x 5 min incubation periods with buffer) with PBS-0.05% Tween 20 and rinsed with PBS. A dilution of commercially available alkaline phosphatase-labeled goat anti-mouse antibody (1:1500 in 2% skim milk in PBS, 100 μL per well) was added to each well. After 1 h of incubation at 37 °C, the plate was washed (3 x 5 min incubation periods with buffer) with PBS-0.05% Tween 20, and rinsed with PBS. A solution of the chromogenic substrate *p*-nitrophenyl phosphate (100 μL per well) at 1 mg/mL in 0.05 M sodium carbonate buffer pH 9.8 containing 10 mM $MgCl_2$ was added. After a 14 h incubation period at 23 °C, the absorbance values were read at 405 nm employing a PowerWave XS plate reader. All samples were prepared in triplicate. The absorbance values were plotted as the percentage inhibition against an increasing concentration of competitor, calculated using wells containing no competitor as the reference point. The values were fitted to a four parameter logistics sigmoidal equation: $y = y_0 + a/[1 + (x/x_0)^b$ using Sigma Plot 10.0.

AUTHOR INFORMATION

Corresponding Author

*Phone: 1519-82442120 ext: 53809; Fax: 1519-7661499; E-mail: fauzanne@uoguelph.ca

Present Addresses

†Apotex Inc**,** 150 Signet Drive, Toronto, Ontario, M9L1T9, Canada

ACKNOWLEDGMENT

This work was supported by the Natural Sciences and Engineering Research Council of Canada. The authors thank Professor S.-I. Hakomori from the Pacific Northwest Research

Institute (Seattle, USA) for the generous gift of mAb SH1 and Dr. E. Samain from the CERMAV (Grenoble, France) for the generous gift of tetrasaccharide **9**.

REFERENCES

1. (a) Slovin, S. F.; Keding, S. J.; Ragupathi, G.; Carbohydrate vaccines as immunotherapy for cancer. *Immunol Cell Biol* **2005,** *83*, 418–428; (b) Yin, Z.; Huang, X.; Recent development in carbohydrate based anticancer vaccines. *J. Carbohydr. Chem.* **2012,** *31*, 143–186.

2. Hakomori, S.-I.; Tumor-associated glycolipid antigens, their metabolism and organization. *Chem. Phys. Lipids* **1986,** *42*, 209–233.

3. (a) Fukushi, Y.; Hakomori, S.; Nudelman, E.; Cochran, N.; Novel fucolipids accumulating in human adenocarcinoma. II. Selective isolation of hybridoma antibodies that differentially recognize mono-, di-, and trifucosylated type 2 chain. *J. Biol. Chem.* **1984,** *259*, 4681–4685; (b) Fukushi, Y.; Hakomori, S.; Shepard, T.; Localization and alteration of mono-, di-, and trifucosyl alpha 1→3 type 2 chain structures during human embryogenesis and in human cancer. *J. Exp. Med.* **1984,** *160*, 506–520; (c) Fukushi, Y.; Kannagi, R.; Hakomori, S.; Shepard, T.; Kulander, B. G.; Singer, J. W.; Location and distribution of difucoganglioside ($VI^3NeuAcV^3III^3Fuc^2NLc^6$) in normal and tumor-tissues defined by its monoclonal-antibody FH6. *Cancer Res.* **1985,** *45*, 3711–3717; (d) Itzkowitz, S. H.; Yuan, M.; Fukushi, Y.; Palekar, A.; Phelps, P. C.; Shamsuddin, A. M.; Trump, B. F.; Hakomori, S.; Kim, Y. S.; $Lewis^x$-related and sialylated $Lewis^x$-related antigen expression in human-malignant and nonmalignant colonic tissues. *Cancer Res.* **1986,** *46*, 2627–2632; (e) Nakasaki, H.; Mitomi, T.; Noto, T.; Ogoshi, K.; Hanaue, H.; Tanaka, Y.; Makuuchi, H.; Clausen, H.; Hakomori, S.; Mosaicism in the expression of tumor-associated carbohydrate antigens in human colonic and gastric cancers. *Cancer Res.*

1989, *49*, 3662–3669; (f) Singhal, A. K.; Ørntoft, T. F.; Nudelman, E.; Nance, S.; Schibig, L.; Stroud, M. R.; Clausen, H.; Hakomori, S.; Profiles of Lewis^x-containing glycoproteins and glycolipids in sera of patients with adenocarcinoma. *Cancer Res.* **1990,** *50*, 1375–1380.

4. (a) Shi, Z. R.; McIntyre, L. J.; Knowles, B. B.; Solter, D.; Kim, Y. S.; Expression of a carbohydrate differentiation antigen, Stage-specific Embryonic Antigen 1, in human colonic adenocarcinoma. *Cancer Res.* **1984,** *44*, 1142–1147; (b) Fox, N.; Damjanov, I.; Knowles, B. B.; Solter, D.; Immunohistochemical localization of the mouse stage-specific embryonic antigen 1 in human tissues and tumors. *Cancer Res.* **1983,** *43*, 669–678; (c) Croce, M. V.; Isla-Larrain, M.; Rabassa, M. E.; Demichelis, S.; Colussi, A. G.; Crespo, M.; Lacunza, E.; Segal-Eiras, A.; Lewis X is highly expressed in normal tissues: a comparative immunohistochemical study and literature revision. *Pathol. Oncol. Res.* **2007,** *13*, 130–138.

5. (a) Asnani, A.; Auzanneau, F.-I.; Synthesis of Lewis X trisaccharide analogues in which glucose and rhamnose replace *N*-acetylglucosamine and fucose, respectively. *Carbohydr. Res.* **2003,** *338*, 1045–1054; (b) Asnani, A.; Auzanneau, F.-I.; Synthesis of Lewis X and three Lewis X trisaccharide analogues in which glucose and rhamnose replace *N*-acetylglucosamine and fucose, respectively. *Carbohydr. Res.* **2008,** *343*, 1653–1664; (c) Hendel, J. L.; Cheng, A.; Auzanneau, F.-I.; Application and limitations of the methyl imidate protection strategy of *N*-acetylglucosamine for glycosylations at O-4: synthesis of Lewis A and Lewis X trisaccharide analogues. *Carbohydr. Res.* **2008,** *343*, 2914–2923.

6. Wang, J.-W.; Asnani, A.; Auzanneau, F.-I.; Synthesis of a BSA-Le^x glycoconjugate and recognition of Le^x analogues by the anti-Le^x monoclonal antibody SH1: The identification of a non-cross reactive analogue. *Bioorg. Med. Chem.* **2010,** *18*, 7174–7185.

7. (a) Imberty, A.; Mikros, E.; Koca, J.; Mollicone, R.; Oriol, R.; Pérez, S.; Computer simulation of histo-blood group oligosaccharides: energy maps of all constituting disaccharides and potential energy surfaces of 14 ABH and Lewis carbohydrate antigens. *Glycoconjugate J.* **1995,** *12*, 331–349; (b) Perez, S.; Mouhous-Riou, N.; Nifant'ev, N. E.; Tsvetkov, Y. E.; Bachet, B.; Imberty, A.; Crystal and molecular structure of a histo-blood group antigen involved in cell adhesion: the Lewis X trisaccharide. *Glycobiology* **1996,** *6*, 537–542; (c) Reynolds, M.; Fuchs, A.; Lindhorst, T. K.; Perez, S.; The hydration features of carbohydrate determinants of Lewis antigens. *Mol. Simul.* **2008,** *34*, 447–460; (d) Miller, K. E.; Mukhopadhyay, C.; Cagas, P.; Bush, C. A.; Solution structure of the Lewis X oligosaccharide determined by NMR spectroscopy and molecular dynamics simulations. *Biochemistry* **1992,** *31*, 6703–6709; (e) Haselhorst, T.; Weimar, T.; Peters, T.; Molecular recognition of Sialyl Lewis^x and related saccharides by two lectins. *J. Am. Chem. Soc.* **2001,** *123*, 10705–10714.

8. (a) Bundle, D. R.; Recognition of carbohydrate antigens by antibody binding sites. In *Bioorganic Chemistry: Carbohydrates*, Hecht, S. M., Ed. Oxford University Press: New York, 1999; pp 370–440; (b) Lemieux, R. U.; How water provides the impetus for molecular recognition in aqueous solution. *Acc. Chem. Res.* **1996,** *29*, 373–380; (c) Woods, R. J.; Computational carbohydrate chemistry: what theoretical methods can tell us. *Glycoconjugate J.* **1998,** *15*, 209–216; (d) Clarke, C.; Woods, R. J.; Gluska, J.; Cooper, A.; Nutley, M. A.; Boons, G.-J.; Involvement of water in carbohydrate−protein Binding. *J. Am. Chem. Soc.* **2001,** *123*, 12238–12247; (e) Laederach, A.; Reilly, P. J.; Modeling protein recognition of carbohydrates. *Proteins: Struct., Funct., Bioinf.* **2005,** *60*, 591–597.

9. Moore, C. J.; Auzanneau, F.-I.; Synthesis of 4” manipulated Lewis X trisaccharide analogues. *Beilstein J. Org. Chem.* **2012,** *8*, 1134–1143.

10. Dumon, C.; Bosso, C.; Utille, J. P.; Heyraud, A.; Samain, E.; Production of Lewis x Tetrasaccharides by Metabolically Engineered Escherichia coli. *ChemBioChem* **2006,** *7*, 359–365.

11. Maaheimo, H.; Kosma, P.; Brade, L.; Brade, H.; Peters, T.; Mapping the binding of synthetic disaccharides representing epitopes of Chlamydial lipopolysaccharide to antibodies with NMR. *Biochemistry* **2000,** *39*, 12778–12788.

12. (a) Bundle, D. R.; Antibody combining sites and oligosaccharide determinants studied by competitive-binding, sequencing and X-Ray crystallography. *Pure Appl. Chem.* **1989,** *61*, 1171–1180; (b) Meikle, P. J.; Young, N. M.; Bundle, D. R.; O-Antigen biotin conjugates - Preparation and use in direct competitive enzyme immunoassays. *J. Immunol. Methods* **1990,** *132*, 255–261; (c) Reimer, K. B.; Gidney, M. A. J.; Bundle, D. R.; Pinto, B. M.; Immunochemical characterization of polyclonal and monoclonal Streptococcus Group-A antibodies by chemically defined glycoconjugates and synthetic oligosaccharides. *Carbohydr. Res.* **1992,** *232*, 131–142.

13. Sheu, S.-Y.; Yang, D.-Y.; Selzle, H. L.; Schlag, E. W.; Energetics of hydrogen bonds in peptides. *Proc. Natl. Acad. Sci. U. S. A.* **2003,** *100*, 12683–12687.

14. Murray-Rust, P.; Stallings, W. C.; Monti, C. T.; Preston, R. K.; Glusker, J. P.; Intermolecular interactions of the C-F bond - the crystallographic environment of fluorinated carboxylic-acids and related Structures. *J. Am. Chem. Soc.* **1983,** *105*, 3206–3214.

15. Vermersch, P. S.; Tesmer, J. J. G.; Quiocho, F. A.; Protein-ligand energetics assessed using deoxy and fluorodeoxy sugars in equilibrium binding and high resolution crystallographic studies. *J. Mol. Biol.* **1992,** *226*, 923–929.

16. Altman, E.; Harrison, B. A.; Hirama, T.; Chandan, V.; To, R.; MacKenzie, R.; Characterization of murine monoclonal antibodies against *Helicobacter pylori* lipopolysaccharide specific for Le^x and Le^y blood group determinants. *Biochemistry and Cell Biology* **2005,** *83*, 589–596.

17. (a) van Roon, A. M. M.; Pannu, N. S.; Hokke, C. H.; Deelder, A. M.; Abrahams, J. P.; Crystallization and preliminary X-ray analysis of an anti-$Lewis^X$ Fab fragment with and without its $Lewis^X$ antigen. *Acta Crystallogr., Sect. D* **2003,** *59*, 1306-1309; (b) van Roon, A.-M. M.; Pannu, N. S.; de Vrind, J. P. M.; van der Marel, G. A.; van Boom, J. H.; Hokke, C. H.; Deelder, A. M.; Abrahams, J. P.; Structure of an anti-Lewis X Fab fragment in complex with its Lewis X antigen. *Structure* **2004,** *12*, 1227–1236; (c) Van Roon, A.-M. M.; Van de Vijver, K. K.; Jacobs, W.; Van Marck, E. A.; Van Dam, G. J.; Hokke, C. H.; Deelder, A. M.; Discrimination between the anti-monomeric and the anti-multimeric Lewis X response in murine schistosomiasis. *Microbes Infect.* **2004,** *6*, 1125–1132.

18. (a) Aspinall, G. O.; Monteiro, M. A.; Pang, H.; Walsh, E. J.; Moran, A. P.; Lipopolysaccharide of the *Helicobacter pylori* type strain NCTC 11637 (ATCC 43504): Structure of the O-antigen chain and core oligosaccharide regions. *Biochemistry* **1996,** *35*, 2489–2497; (b) Aspinall, G. O.; Monteiro, M. A.; Shaver, R. T.; Kurjanczyk, L. A.; Penner, J. L.; Lipopolysaccharides of *Helicobacter Pylori* serogroups O:3 and O:6 structures of a class of lipopolysaccharides with reference to the location of oligomeric units of D-Glycero-α-D-Manno-heptose residues. *Eur. J. Biochem.* **1997,** *248*, 592–601; (c) Monteiro, M. A.; Appelmelk, B. J.; Rasko, D. A.; Moran, A. P.; Hynes, S. O.; MacLean, L. L.; Chan, K. H.; Michael, F. S.; Logan, S. M.; O'Rourke, J.; Lee, A.; Taylor, D. E.; Perry, M. B.; Lipopolysaccharide structures of *Helicobacter pylori* genomic strains 26695 and J99, mouse model *H. pylori* Sydney strain,

H. pylori P466 carrying sialyl Lewis X, and *H. pylori* UA915 expressing Lewis B. *Eur. J. Biochem.* **2000,** *267*, 305–320.

19. Appelmelk, B. J.; Simoons-Smit, I.; Negrini, R.; Moran, A. P.; Aspinall, G. O.; Forte, J. G.; De Vries, T.; Quan, H.; Verboom, T.; Maaskant, J. J.; Ghiara, P.; Kuipers, E. J.; Bloemena, E.; Tadema, T. M.; Townsend, R. R.; Tyagarajan, K.; Crothers, J. M.; Monteiro, M. A.; Savio, A.; De Graaff, J.; Potential role of molecular mimicry between *Helicobacter pylori* lipopolysaccharide and host Lewis blood group antigens in autoimmunity. *Infect. Immun.* **1996,** *64*, 2031–2040.

20. (a) Weiss, J. B.; Strand, M.; Characterization of developmentally regulated epitopes of *Schistosoma mansoni* egg glycoprotein antigens. *J. Immunol.* **1985,** *135*, 1421–1429; (b) Srivatsan, J.; Smith, D. F.; Cummings, R. D.; The human blood fluke *Schistosoma mansoni* synthesizes glycoproteins containing the Lewis X antigen. *J. Biol. Chem.* **1992,** *267*, 20196–20203; (c) Wuhrer, M.; Dennis, R. D.; Doenhoff, M. J.; Lochnit, G.; Geyer, R.; *Schistosoma mansoni* cercarial glycolipids are dominated by Lewis X and pseudo-Lewis Y structures. *Glycobiology* **2000,** *10*, 89–101; (d) Remoortere, A. v.; H.Hokke, C.; Dam, G. J. v.; Die, I. v.; M.Deelder, A.; Eijnden, D. H. v. d.; Various stages of *Schistosoma* express Lewis^x, LacdiNAc, GalNAcβ1–4(Fucα1–3)GlcNAc and GalNAcβ1–4(Fucα1–2Fucα1–3)GlcNAc carbohydrate epitopes: detection with monoclonal antibodies that are characterized by enzymatically synthesized neoglycoproteins. *Glycobiology* **2000,** *10*, 601–609; (e) Khoo, K.-H.; Huang, H.-H.; Lee, K.-M.; Characteristic structural features of schistosome cercarial N-glycans: expression of Lewis X and core xylosylation. *Glycobiology* **2001,** *11*, 149–163; (f) Huang, H.-H.; Tsai, P.-L.; Khoo, K.-H.; Selective expression of different fucosylated epitopes on two distinct sets of

Schistosoma mansoni cercarial O-glycans: identification of a novel core type and Lewis X structure. *Glycobiology* **2001,** *11*, 395–406.

21. Hendel, J. L.; Auzanneau, F.-I.; Convergent preparation of dimLe^x hexasaccharide analogues. *Eur. J. Org. Chem.* **2011**, 6864–6876.

22. Dubois, M.; Gilles, K. A.; Hamilton, J. K.; Rebers, P. A.; Smith, F.; Colorimetric Method for Determination of Sugars and Related Substances. *Anal. Chem*. **1956,** *28*, 350–356.

TOC- graphics.